IAI Journals.ASM.org

Influenza A Virus Alters Pneumococcal Nasal Colonization and Middle Ear Infection Independently of Phase Variation

John T. Wren, Lance K. Blevins, Bing Pang, Lauren B. King, Antonia C. Perez, Kyle A. Murrah, Jennifer L. Reimche, Martha A. Alexander-Miller, W. Edward Swords

Department of Microbiology and Immunology, Wake Forest School of Medicine, Winston-Salem, North Carolina, USA

Streptococcus pneumoniae **(pneumococcus) is both a widespread nasal colonizer and a leading cause of otitis media, one of the most common diseases of childhood. Pneumococcal phase variation influences both colonization and disease and thus has been linked to the bacteria's transition from colonizer to otopathogen. Further contributing to this transition, coinfection with influenza A virus has been strongly associated epidemiologically with the dissemination of pneumococci from the nasopharynx to the middle ear. Using a mouse infection model, we demonstrated that coinfection with influenza virus and pneumococci enhanced both colonization and inflammatory responses within the nasopharynx and middle ear chamber. Coinfection studies were also performed using pneumococcal populations enriched for opaque or transparent phase variants. As shown previously, opaque variants were less able to colonize the nasopharynx. *In vitro*, this phase also demonstrated diminished biofilm viability and epithelial adherence. However, coinfection with influenza virus ameliorated this colonization defect *in vivo*. Further, viral coinfection ultimately induced a similar magnitude of middle ear infection by both phase variants. These data indicate that despite inherent differences in colonization, the influenza A virus exacerbation of experimental middle ear infection is independent of the pneumococcal phase. These findings provide new insights into the synergistic link between pneumococcus and influenza virus in the context of otitis media.**

Otitis media (OM) is among the most common diseases of childhood, affecting most children at least once before the age of 3 years and accounting for billions of dollars in health care expenditures annually in the United States alone (1, 2). *Streptococcus pneumoniae* (pneumococcus) is the most commonly isolated pathogen of OM even following the advent of widespread vaccination with the pneumococcal conjugate vaccine (3). Pneumococci can also asymptomatically colonize the nasopharynx (4–7). There remains much to be learned regarding the factors contributing to the transition from carriage to OM disease.

Epidemiologic evidence strongly indicates a role for upper respiratory tract viruses, particularly influenza A virus (IAV), in the dissemination of *S. pneumoniae* from its nasopharyngeal niche to the middle ear (7–11). Indeed, experimental IAV infection of human volunteers was shown to increase both nasal pneumococcal burden and incidence of OM (12, 13). This synergistic interaction has also been observed across different pneumococcal strains and serotypes in ferrets (14) and, extensively, in chinchillas (15, 16). The development of mouse models, though often requiring either the use of artificial or invasive procedures (17, 18) or infant mice (19–21), has further significantly contributed to and widened the field. Largely stemming from these models, the viral factors which predispose to OM are well-studied and include eustachian tube dysfunction, ciliary dysmotility, mucosal inflammation, and neutrophil impairment (8, 11, 22–24). How this viral predisposition affects specific pneumococcal subpopulations during middle ear infection, however, is less well understood.

S. pneumoniae is a tremendously variable pathogen that is well adapted to persist within the human nasopharyngeal microbiota. In addition to including numerous capsular types, pneumococcal populations also undergo intrastrain phase variation in which bacteria spontaneously and reversibly shift between opaque and transparent colony types (25). Present data indicate that pneumococci exist in humans as a heterogeneous combination of these phases during both colonization and disease (26). In prior studies, the transparent phase was shown to be more efficient in nasopharyngeal colonization *in vivo* (25), along with increased adherence to activated lung epithelial cells *in vitro* (27) and an increase in transparent-phase pneumococci within biofilm communities (28). Biofilms are surface-attached bacterial communities that are encased in an extracellular matrix and display an altered metabolic phenotype (29). These structures in particular have previously been linked both clinically and experimentally to nasal colonization and OM (30–32). The opaque phase, in contrast, is associated with invasive disease (25), with increased resistance to opsonophagocytosis and host clearance (33), likely mediated through increased capsular expression (34).

We hypothesized that coinfection with IAV may alter pneumococcal colonization and, possibly, alter the dynamics of middle ear infection by the two phases, disrupting this traditional paradigm regarding the transparent and opaque phases. Previous work in a chinchilla model has indicated that, at later time points, opaque-phase variants predominated in both the nasopharynx and middle ear following IAV infection (35). As the opaque phase is not traditionally associated with colonization in animal models (25) or in humans (26), this current study was designed to further investigate the interaction of IAV and the two phases of *S. pneumoniae* in

Received 2 July 2014 **Returned for modification** 9 August 2014
Accepted 20 August 2014
Published ahead of print 25 August 2014
Editor: A. Camilli
Address correspondence to W. Edward Swords, wswords@wakehealth.edu.

doi:10.1128/IAI.01856-14

a distinct animal model and using a well-studied colonizing pneumococcal strain.

To investigate our hypothesis, we first aimed to develop a readily accessible adult mouse model of nasal colonization and middle ear infection that mimicked the natural course of infection. Therefore, we utilized an intranasal inoculation of a colonizing pneumococcal strain (EF3030) that has been shown to colonize the mouse nasopharynx in the absence of lethal, systemic disease (36, 37). We found that a preceding infection with IAV enhanced nasal colonization by *S. pneumoniae*, and this was correlated with a significant increase in middle ear infection. We then employed this model to investigate whether viral coinfection altered the pathogenesis of middle ear infection by the two pneumococcal phases. Our results demonstrated inherent differences in bacterial adherence to nasopharyngeal epithelial cells and biofilm viability *in vitro* as well as nasal colonization *in vivo* between the two phases. Despite this, IAV coinfection ultimately enabled both phases to colonize the nasopharynx and infect the middle ear similarly. This provided evidence that the pathogenesis of pneumococcal colonization and middle ear infection during IAV coinfection was phase independent.

MATERIALS AND METHODS

Infectious agents and growth conditions. *S. pneumoniae* EF3030 (serotype 19F) is a nasopharyngeal isolate that has previously been shown to colonize the mouse nasopharynx in the absence of lethal, systemic disease (36, 37). Pneumococci were cultured on Trypticase soy agar (Becton, Dickinson and Co.) with 5% sheep blood (Hemostat Laboratories) and 4 μg/ml gentamicin (Sigma). For freezer stocks, *S. pneumoniae* bacteria were grown in brain heart infusion (BHI) broth (Becton, Dickinson and Co.) supplemented with 10% heat-inactivated horse serum and 10% catalase (2,500 U/ml; Worthington) until mid-late logarithmic phase (optical density at 600 nm [OD_{600}] of 0.6 to 0.85), diluted 1:1 in 50% glycerol, and frozen at −80°C. Influenza A/PR/8/34-GFP (PR8/34-GFP, where GFP is green fluorescent protein) (H1N1) used in this study was generously provided by Adolfo García-Sastre (38). Viral stocks were prepared in embryonated eggs, and titers were determined as the median tissue culture infectious dose ($TCID_{50}$) in Madin-Darby canine kidney cells.

Phase determination and variant isolation. Colony phenotype was determined under oblique light, as described previously (25, 39). Phase variants of the parent EF3030 strain were isolated prior to each experiment and were confirmed to contain >90% of colonies in the same phase of at least 100 counted colonies. These variants retained the ability to shift between the transparent and opaque phases. The percent opacity of each inoculum was confirmed prior to each experiment.

Coinfection model. Female, 6-week-old BALB/c mice (Jackson Laboratory) were housed in a biosafety level 2 (BSL-2) facility. All mouse infection protocols were approved by the Wake Forest University Health Sciences Institutional Animal Care and Use Committee. Mice were anesthetized with 2,2,2-tribromoethanol (Avertin; 20 mg/ml) (Acros Organics) intraperitoneally and infected intranasally with 3×10^3 $TCID_{50}$s of IAV diluted in 20 μl of sterile phosphate-buffered saline (PBS) on ice or with an equal volume of vehicle control. Four days later, mice were again anesthetized and inoculated intranasally with 5×10^6 CFU of *S. pneumoniae* in 20 μl of BHI broth on ice or in vehicle control. Bacterial density was confirmed by serial dilution and plate count. The phase composition of each inoculum was also confirmed. Mice were weighed and assessed for disease at least twice daily. While minimal and moderate signs of disease were apparent in mice inoculated with EF3030 alone and IAV alone, respectively, a small subset of coinfected mice (<10%) exhibited moribund disease. These mice were euthanized on that day. At days 2 and 4 postbacterial infection, mice were euthanized, and the nasopharynx and bilateral bullae were aseptically excised and homogenized (PowerGen 100; Fisher Scientific) in sterile PBS. Aliquots of these homogenates were serially diluted and plated for bacterial quantification and phase determination following 20 h of incubation at 37°C and 5% CO_2.

qRT-PCR. Tissue homogenates were snap-frozen and stored at −80°C. Aliquots were then subjected to three freeze-thaw cycles, and RNA was isolated with TRIzol reagent (Ambion) and reverse transcribed to cDNA using random primers (Invitrogen), deoxynucleoside triphosphates (Promega), and Superscript III reverse transcriptase (Invitrogen) supplemented with RNasin (Promega) according to each manufacturer's specifications. Influenza virus RNA was then detected by real-time quantitative reverse transcription-PCR (qRT-PCR) using TaqMan Universal PCR master mix (Applied Biosystems) and IAV primers (40) with a 7500 Real-Time PCR System (Applied Biosystems), essentially as described previously (41).

Histopathology. Excised nasopharynges and bullae from preselected mice were fixed in 4% paraformaldehyde, decalcified, embedded in 22-oxacalcitriol (O.C.T. solution; Sakura Finetek), and sequentially frozen by being placed at room temperature for 3 h, at −20°C for 12 h, and at −80°C for 24 h or until ready for use. Samples were cryosectioned into approximately 5-μm slices, stained with hematoxylin and eosin, mounted with Permount (Electron Microscopy Sciences), and examined microscopically.

Adherence assay. The human nasopharyngeal carcinoma cell line Detroit 562 (ATCC CCL-138) was maintained in Eagle's minimal essential medium with L-glutamine, 10% heat-inactivated fetal bovine serum, 100 U/ml penicillin, and 100 μg/ml streptomycin (Gibco). Cells were grown in T75 flasks (Corning) at 37°C and 5% CO_2. Adherence assays were performed essentially as described previously (28, 42). Approximately 2×10^5 cells/well were seeded onto 24-well flat-bottom, tissue culture-treated plates (Costar) and allowed to grow to confluence (~4×10^5 cells/well). When cells were ready to infect, bacteria were grown in BHI broth supplemented with 2,500 U/ml catalase to mid-logarithmic phase (OD_{600} of 0.45 to 0.65). Cell monolayers were washed three times in warmed Dulbecco's PBS (DPBS; Lonza) and overlaid with 1 ml/well serum- and antibiotic-free medium containing 1×10^7 CFU of *S. pneumoniae* opacity variants. The bacterial density and phase composition of each inoculum were determined. To initiate bacterial-epithelial cell interactions, the plates were centrifuged at 1,300 × *g* for 5 min and then incubated at 37°C and 5% CO_2 for 1 h. Following incubation, the monolayer was washed three times with DPBS to remove nonadherent bacteria. Epithelial cells and adherent bacteria were then dissociated from the plate by treatment with 0.25% trypsin-EDTA (Gibco) for 10 min. The number of adherent bacteria was determined by serial dilution and plate count. Pneumococcal adhesion was expressed as percent adherence relative to the inoculum. The experiment contained three biological replicates per opacity variant and included six variants of each phase.

Static biofilm assay. This assay was performed essentially as described previously (43). Briefly, *S. pneumoniae* opacity variants were inoculated into Todd-Hewitt broth (Becton-Dickinson) with 0.5% yeast extract (Difco) and supplemented with 10% heat-inactivated horse serum and 2,500 U/ml catalase and were seeded onto 24-well flat-bottom plates (Costar) at 5×10^5 CFU/well. The bacterial density and phase composition of each inoculum were confirmed prior to each experiment. After incubation at 37°C and 5% CO_2 for 4 or 24 h, the medium was removed, and the adherent biofilms were resuspended in sterile PBS by scraping and vigorous pipetting. The biofilm viability, defined as the total recovered numbers of surface-attached *S. pneumoniae* bacteria, and phase composition were then determined via plate count and phase determination, respectively. Each experiment contained three biological replicates and was repeated at least three times.

Statistical analysis. Pairwise comparisons of nasal colonization, middle ear infection, and phase composition were analyzed by a Mann-Whitney *U* test. The percent adherence of pneumococcal phase variants to epithelial cells and *in vitro* biofilm viability were analyzed by Student's *t* test. The correlation between nasal colonization density and middle ear

TABLE 1 Presence of IAV RNA in the nasopharynx and middle ear

Tissue type and inoculum	% tissue containing IAV RNA (SE) at:[a] Day 2	Day 4
Nasopharynx		
IAV	100.0 (0.0)	88.9 (16.6)
IAV and *S. pneumoniae*	76.9 (28.4)	75.0 (33.4)
Middle ear		
IAV	27.8 (13.8)	0.0 (0.0)
IAV and *S. pneumoniae*	15.4 (10.0)	0.0 (0.0)

[a] The percentage of tissues that contained detectable IAV RNA by qRT-PCR at the indicated time point post-bacterial infection. Days 2 and 4 correspond to day 6 and day 8 post-viral infection, respectively. Data were pooled from two replicate experiments. Data were evaluated via Fisher's exact test, and no significant differences between IAV- and coinfected tissues were present ($P > 0.05$).

bacterial burden was assessed by Spearman's rank correlation test. Where noted in the text, fold change was calculated using the geometric mean, except for biofilm viability, which was calculated using the arithmetic mean. Samples for which the bacterial counts were below the limit of detection were considered uninfected. For statistical analysis and graphing, these points were plotted at the limit of detection. A P value of <0.05 was considered to be significant. Statistical analyses were performed using GraphPad Prism, version 5.01 (GraphPad Software).

RESULTS

Nasal colonization is increased by prior influenza virus infection. Mice were infected intranasally with IAV and 4 days later infected with *S. pneumoniae* to investigate the effect of antecedent viral infection on pneumococcal colonization. The mouse nasopharynx was permissive to IAV infection as influenza viral RNA was still detectable in 75 to 89% of mice by day 8 post-viral infection (Table 1). Further, all mice challenged with *S. pneumoniae* exhibited nasal colonization at both days 2 and 4 post-bacterial infection (Fig. 1A). This colonization was observed to persist for at least 20 days (data not shown). In mice coinfected with IAV and *S. pneumoniae*, the magnitude of pneumococcal colonization was significantly increased by ~8-fold at both days 2 and 4 ($P = 0.0003$ and $P = 0.0043$, respectively) (Fig. 1A). Bacterial coinfection, alternatively, did not have a significant effect on the proportion of IAV-infected nasopharynges ($P > 0.05$, Fisher's exact test) (Table 1).

Influenza virus enhances pneumococcal middle ear infection. In children, the magnitude of nasal colonization is linked to the incidence of OM (44). We next aimed to determine whether the increase in nasal pneumococcal colonization following IAV infection was similarly associated with middle ear infection. IAV coinfection significantly increased the middle ear pneumococcal burden by nearly 40-fold at both days 2 and 4 post-bacterial infection ($P < 0.0001$ and $P = 0.025$, respectively) (Fig. 1B). Prior viral infection also altered the incidence of middle ear bacterial infection as 100% of coinfected mice possessed detectable numbers of bacteria in the normally sterile middle ear space of at least one ear, whereas detectable numbers of bacteria were present in 75% of singly infected mice ($P = 0.01$; Fisher's exact test). These coinfected mice were also more prone to develop bilateral middle ear infection (88% versus 35%, respectively, for coinfection versus single infection; $P = 0.0004$, Fisher's exact test) (data not shown), a frequently used clinical criterion for the initiation of antimicrobial therapy (45). Further, the magnitude of middle ear infection was found to be directly correlated to the density of nasal pneumococcal colonization density but only during coinfection with IAV (Fig. 1C), echoing clinical data (44).

Using the presence of IAV RNA in the middle ear as a surrogate marker for viral infection at that site, coinfection with pneumococci had no effect on the proportion of ears infected with IAV ($P > 0.05$, Fisher's exact test) (Table 1). The middle ear pneumococcal burden, however, was significantly elevated in coinfected mice even in ears without detectable IAV RNA ($P < 0.01$) (Fig. 1D). Further, the pneumococcal burden in the middle ears that did contain IAV RNA at the designated time points was significantly greater than that both in ears from singly infected mice and in ears from coinfected mice that did not contain viral RNA ($P < 0.01$) (Fig. 1D).

Influenza virus induces increased nasal epithelial inflammation. IAV-induced inflammation in the middle ear has previously been shown to propagate pneumococcal OM (21). To determine whether IAV induced a similar effect in the nasopharynx, nasal sections from both singly infected and coinfected mice were compared using histopathologic staining and microscopic analyses. The nasal epithelium from mock-infected mice was intact and contained a thick mucociliary border (Fig. 2, Mock). During colonization with *S. pneumoniae*, an inflammatory infiltrate was present within the nasal meatuses consisting primarily of cells morphologically resembling neutrophils (Fig. 2, *S. pneumoniae*), as has been noted previously (46). Despite this infiltrate, the nasal epithelium was largely unchanged from that of mock-infected mice with the notable exceptions of isolated areas of ciliary denudation and areas of increased mucus production (Fig. 2, *S. pneumoniae*). In contrast, IAV infection, both in the presence and absence of *S. pneumoniae*, was associated with substantial damage to the nasal epithelium, including widespread ciliary denudation, epithelial disruption, areas of microvascular hemorrhage, and exposure of the lamina propria (Fig. 2, IAV and *S. pneumoniae* + IAV). Epithelial changes appeared similar between IAV-only and coinfected mice. A predominantly neutrophilic infiltrate was again present within the lumen of the nasal meatuses of both IAV-only (Fig. 2, IAV) and coinfected mice (Fig. 2, *S. pneumoniae* + IAV). Unlike the infiltrate in mice colonized with pneumococci alone, this infiltrate was also epithelium associated (Fig. 2, IAV and *S. pneumoniae* + IAV). These data indicate that IAV alters the nasopharyngeal epithelium, suggesting a potential mechanism by which nasal colonization is enhanced following viral infection.

Middle ear inflammation is increased in coinfected mice. As pneumococci were detected in the middle ears of both singly infected and coinfected mice, middle ear sections were evaluated histopathologically to determine whether the increased bacterial burden was associated with increased inflammation or signs of disease. No evidence of inflammation or infiltrate was observed in mock-infected mice (Fig. 3, Mock). A minimal inflammatory infiltrate was occasionally present in mice infected with *S. pneumoniae* alone. Of note, one ear was observed to contain a large inflammatory infiltrate within the lumen. In most cases, however, the tissues appeared similar to those of mock-infected mice (Fig. 3, *S. pneumoniae*), as has been described previously (20). The heterogeneity of these findings is likely attributable to the high variability of bacterial burden that we detected in the ears of singly infected mice. While most values were clustered around ~10^2 to 10^3 CFU/ml, the range extended to as high as ~10^6 CFU/ml (Fig. 1B).

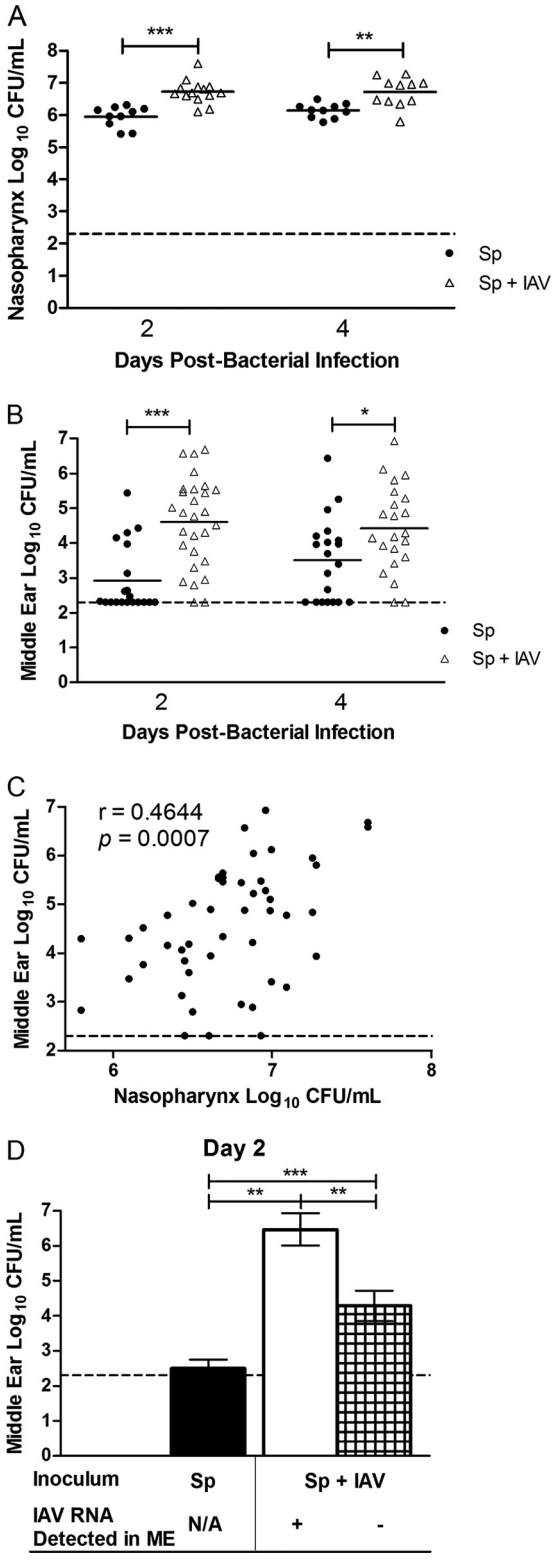

FIG 1 Influenza A virus exacerbates nasal colonization and middle ear infection by *S. pneumoniae*. Mice were infected intranasally with influenza A virus (IAV) PR8/34-GFP and 4 days later infected with *S. pneumoniae* (Sp) EF3030. Graphs show the magnitude of nasal colonization (A) and middle ear infection (B) by *S. pneumoniae* in the tissue homogenates from days 2 and 4 post-bacterial infection (corresponding to days 6 and 8 post-viral infection). Each data point represents a single nasopharynx or ear, and the data are pooled from two replicate experiments. The short, solid horizontal lines denote the geometric mean, and the horizontal dotted line represents the limit of detection of the assay. Statistical analysis was performed using a two-tailed Mann-Whitney *U* test (*, $P < 0.05$; **, $P < 0.01$; ***, $P < 0.001$). (C) Correlation between nasal colonization density of *S. pneumoniae* and the middle ear pneumococcal burden in coinfected mice. Each ear is correlated to its respective nasopharynx. The data contain both time points and are pooled from two replicate experiments. Statistical analysis was performed using Spearman's rank correlation test and is denoted by Spearman's rank correlation coefficient (r) and P value. (D) Middle ear (ME) pneumococcal burden at day 2 post-bacterial infection in mice infected with *S. pneumoniae* alone (black bar), coinfected with IAV and possessing detectable viral RNA in the middle ear (white bar), or coinfected with IAV but containing no detectable viral RNA in the middle ear (hatched bar) from a separate experiment. Each bar represents the geometric mean ± 95% confidence intervals. The presence of IAV RNA was detected by qRT-PCR, and no IAV RNA was detectable in the middle ear by day 4 post-bacterial infection (day 8 post-viral infection). Data are pooled from two replicate experiments. Statistical analysis was performed using a two-tailed Mann-Whitney *U* test (**, $P < 0.01$; ***, $P < 0.001$). N/A, not applicable.

As middle ear inflammatory infiltrates have been shown to correlate with bacterial burden (47), it is likely that the disparate finding that we observed in one ear was due to an abnormally high magnitude of middle ear infection in that animal.

In mice infected with IAV alone, an inflammatory infiltrate was also largely absent. However, there was evidence of mucosal inflammation with increased edema, epithelial thickening, and vasodilation (Fig. 3, IAV). These findings were more prominent in coinfected mice (Fig. 3, *S. pneumoniae* + IAV). Further, an inflammatory infiltrate consisting primarily of neutrophils was readily apparent in the middle ear lumens of coinfected mice (Fig. 3, *S. pneumoniae* + IAV). Taken together, these results indicate that the increased magnitude of middle ear bacterial infection following IAV was associated with increased evidence of both mucosal inflammation and inflammatory infiltration. As these are two histological findings linked to the clinical diagnosis of OM (48), these data are suggestive that middle ear disease was likewise increased during bacterial-viral coinfection in these mice.

During coinfection, the transparent phase is found more frequently in the nasopharynx; the opaque phase is found more frequently in the middle ear. Pneumococci exhibit phase variation between a transparent phase associated more with nasal colonization and an opaque phase associated more with disease (25). To determine whether this association was also present during bacterial-viral coinfection, the phase composition of colonies isolated from mice inoculated with IAV and *S. pneumoniae* was assessed. The pneumococcal strain used in this study, EF3030, was comprised of a heterogeneous combination of both phases, as occurs naturally in humans (26). This strain was confirmed to contain approximately 73% opaque-phase colonies at the time of inoculation. The propensity of the transparent and opaque phases to be isolated from the nasopharynx and ear, respectively, persisted *in vivo* during coinfection with IAV. By day 4, colonies isolated from the nasopharynx were more transparent while those from the middle ear were more opaque ($P = 0.037$) (Table 2), reflecting a similar study in children with acute OM (26). Of note, a similar comparison could not be made in singly infected mice as insufficient bacterial counts to evaluate phase composition were consistently isolated from the middle ears of these mice.

Transparent-phase pneumococci are more adherent to nasopharyngeal epithelial cells. Since transparent-phase pneumococci were isolated more frequently from the nasopharynges of

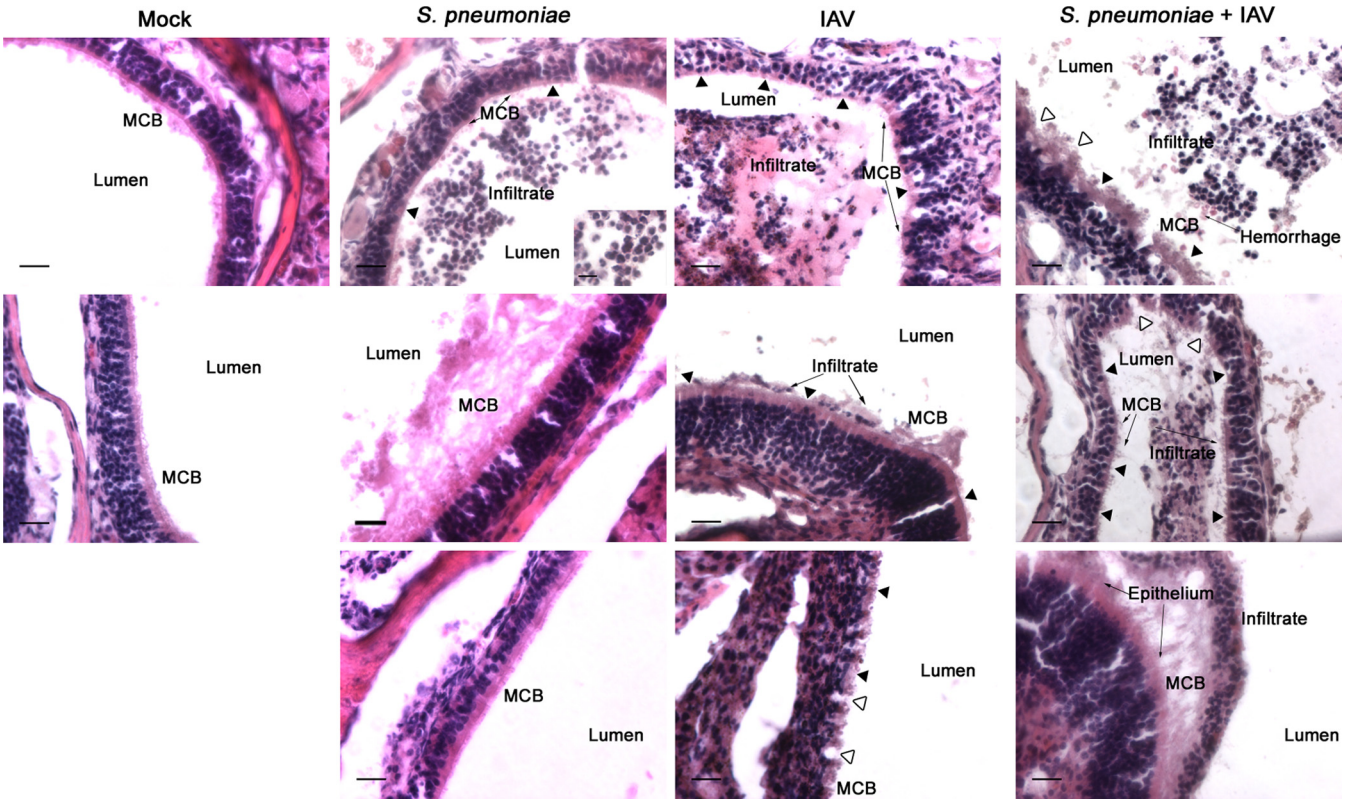

FIG 2 Influenza virus induces nasal epithelial changes. Representative histological images of the lateral wall of the nasal cavity from mice ($n \geq 4$) infected intranasally with influenza A virus (IAV) and 4 days later infected by *S. pneumoniae* from both days 2 and 4 post-bacterial infection (corresponding to days 6 and 8 post-viral infection). Representative images from mock-infected mice and mice infected with *S. pneumoniae* alone or IAV alone are also shown. Tissues were stained with hematoxylin and eosin and examined microscopically at a magnification of ×40. Scale bar, 20 μm. Areas in the insets were examined at a magnification of ×60 (scale bar, 10 μm). Relevant structures are labeled, including the mucociliary border (MCB). Filled arrowheads mark areas of ciliary denudation; open arrowheads indicate areas of epithelial disruption.

both singly infected and coinfected mice, we hypothesized that this may be mediated by increased epithelial adherence. To test this, phase variants of EF3030 were generated and were confirmed to contain >90% of colonies in the same phase. Transparent-phase pneumococci of this strain demonstrated significantly increased adherence to Detroit 562 cells, a human nasopharyngeal carcinoma cell line, than their opaque counterparts (41.1% versus 25.4%, respectively; $P = 0.002$) (Fig. 4A). Of note, Cundell et al. previously reported increased adherence by the transparent phase to activated but not resting A549 immortalized alveolar epithelial cells (27). As invasive blood isolates were employed in the prior study, this discrepancy is likely attributable to differences in the pneumococcal strains studied.

Biofilm viability is enhanced in transparent-phase pneumococci. To further explore potential mechanisms to explain why the transparent phase was isolated more frequently from the nasopharynx in this model, we investigated biofilm viability *in vitro*. Biofilms are critical for nasal colonization and persistence in both animal models and children (31, 49). Further, bacterial adherence is the essential first step in biofilm formation. As such, we hypothesized that a transparent-phase variant of EF3030 would also exhibit enhanced biofilm viability along with increased adherence. In an *in vitro* biofilm model, we found that biofilm viability, defined as the numbers of surface-attached pneumococci, was significantly increased in the transparent variant by 3.5-fold at 4 h and 3-fold at 24 h ($P = 0.0002$ and $P = 0.0002$, respectively) (Fig. 4B). In the time frame studied, no significant phase shifting of the phase variants during biofilm formation was observed (data not shown). These results indicated not only that biofilm formation selects for the transparent phase from a mixed-phase inoculum, as has been noted previously (28), but also that transparent-phase pneumococci themselves demonstrate increased *in vitro* biofilm viability independent of phase shifting.

Coinfection with influenza virus ablates the nasal colonization defect of opaque-phase pneumococci. The opaque phase is noted for both its increased invasiveness and its impaired ability to colonize the nasopharynx (25). This phenotype is likely linked, in part, to the reduced adherence and biofilm viability in this phase that we observed *in vitro*. Theoretically, this impairment in nasal colonization ability could serve as a natural check by limiting the number of the opaque phase bacteria in the nasopharynx, thereby inhibiting pneumococci from too rapidly killing its host. As such, we aimed to determine whether the IAV enhancement of pneumococcal colonization indicated by the data Fig. 1A extended to opaque-phase pneumococci, potentially disrupting a delicate balance. To investigate this, phase variants that were confirmed prior to each experiment to contain >90% of colonies in the same phase were inoculated into mice either alone or 4 days following IAV infection. The variants used in this study are not "locked," thereby allowing us to assess whether the viral coinfection altered phase

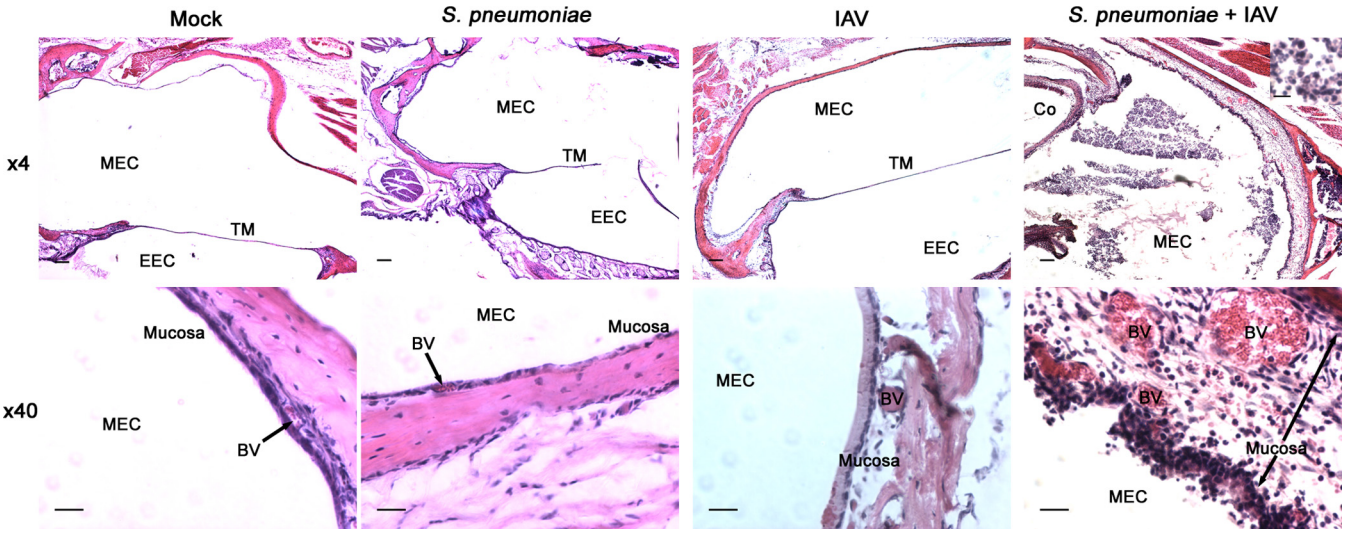

FIG 3 Middle ear inflammation and infiltrate are increased during coinfection. Representative histological images of the middle ear ($n \geq 8$) from mice infected intranasally with influenza A virus (IAV) and 4 days later infected by *S. pneumoniae* from both days 2 and 4 post-bacterial infection (corresponding to days 6 and 8 post-viral infection). Representative images from mock-infected mice and mice infected with *S. pneumoniae* alone or IAV alone are also shown. Tissues were stained with hematoxylin and eosin. The samples were examined microscopically at magnifications of ×4 and ×40, and the scale bars represent 100 μm and 20 μm, respectively. Areas in the insets were examined at a magnification of ×60 (scale bar, 10 μm). Relevant structures are labeled, including the middle ear cavity (MEC), tympanic membrane (TM), external ear canal (EEC), and blood vessels (BV).

shifting *in vivo*. Confirming prior studies (25), the opaque-phase variant when used alone for infection exhibited impaired colonization relative to the transparent variant although this was statistically significant only at day 2 ($P = 0.005$) (Fig. 5A). Prior viral

TABLE 2 Percent opacity of colonies isolated from IAV- and coinfected mice

S. pneumoniae strain or variant and infection program (% opaque-phase colonies in inoculum)[b]	% opaque-phase colonies (SE)[a]			
	Day 2[c]		Day 4	
	Nasopharynx	Middle ear	Nasopharynx	Middle ear
Parent strain (73.0)				
Single infection	69.5 (3.4)		64.8 (5.0)	
IAV coinfection	64.1 (4.0)	72.2 (5.5)	62.0 (5.8)	77.9 (4.5)*
Opaque variant (99.4)				
Single infection	99.5 (0.2)		98.4 (0.6)	
IAV coinfection	96.1 (1.4)	98.1 (0.8)	99.8 (0.1)†	100.0 (0.0)
Transparent variant (5.0)				
Single infection	9.1 (2.0)		6.8 (2.3)	
IAV coinfection	7.6 (1.2)	22.8 (4.5)**	9.6 (1.8)	26.4 (8.2)

[a] Data represent the mean percentages of opaque-phase colonies isolated from either the nasopharynx or middle ear of singly infected or coinfected mice at the indicated time points from two pooled experiments. The percentage was calculated as follows: (number of opaque-phase colonies/total number of colonies) × 100. Insufficient numbers of CFUs were isolated from the middle ears of singly infected mice to assess the percentage of opaque colonies. *, $P < 0.05$; **, $P < 0.01$ (compared to the respective nasopharynx by a Mann-Whitney *U* test); †, $P < 0.05$ (compared to respective *S. pneumoniae*-only inoculated mice by a Mann-Whitney *U* test).

[b] *S. pneumoniae* strain EF3030 was used for single infections and for coinfection with IAV.

[c] Days 2 and 4 are the days post-bacterial infection, corresponding to days 6 and 8 post-viral infection, respectively.

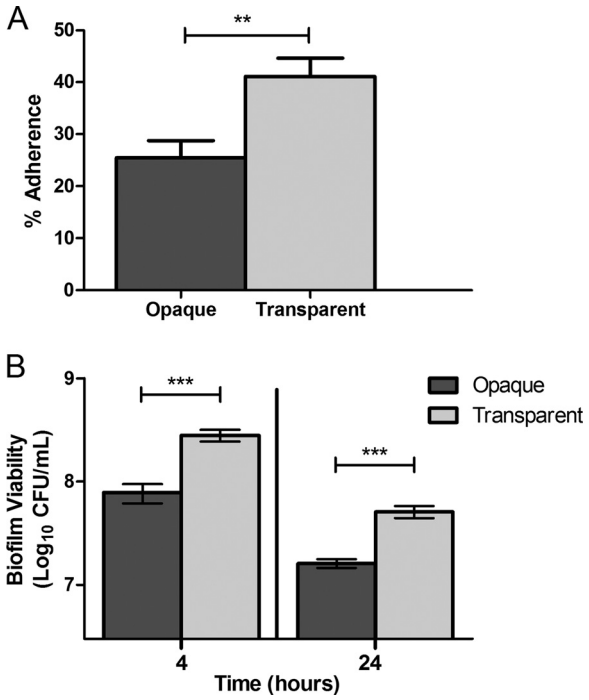

FIG 4 The transparent phase displays enhanced epithelial adherence and biofilm viability *in vitro*. (A) Adherence of *S. pneumoniae* opacity variants to Detroit 562 nasopharyngeal epithelial cells after 60 min, expressed as the percentage of adherent bacteria relative to the inoculum. Bars represent the means ± standard errors of the means. The experiment was performed with three biological replicates per opacity variant and six variants of each phase. Statistical analysis was performed using a two-tailed Student's *t* test (**, $P < 0.01$). (B) Viability of pneumococcal opacity variants from 4- and 24-h static biofilms. Bars represent the means ± standard errors of the means of three replicate experiments. Statistical analysis was performed using a two-tailed Student's *t* test (**, $P < 0.01$; ***, $P < 0.001$).

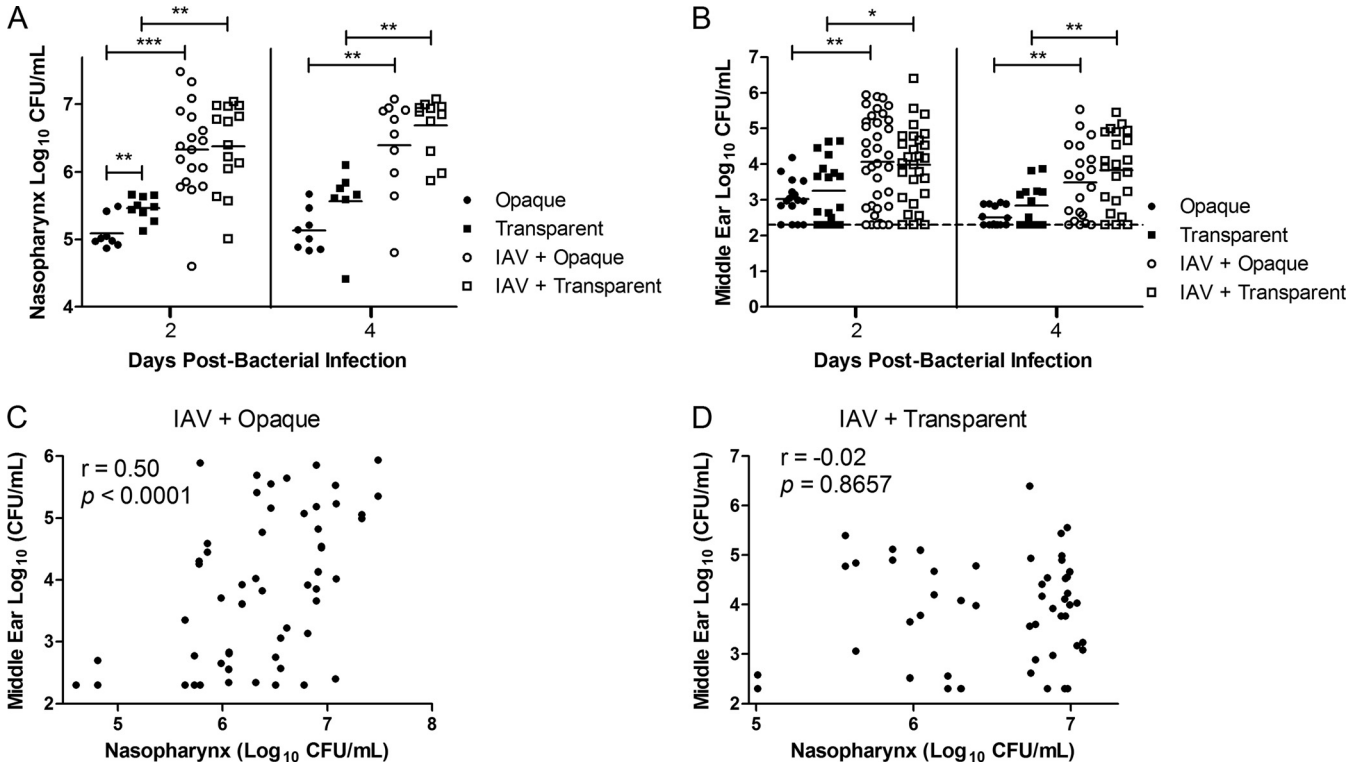

FIG 5 Coinfection with influenza virus alters nasal colonization and middle ear infection by both the opaque and transparent phases. Mice that had been either mock infected or infected intranasally with influenza A virus (IAV) 4 days prior were infected with either the opaque- or transparent-phase variant of *S. pneumoniae* EF3030. Graphs show the magnitude of nasal colonization (A) and middle ear infection (B) by *S. pneumoniae* in the tissue homogenates from days 2 and 4 post-bacterial infection (corresponding to days 6 and 8 post-viral infection). Each data point denotes a single nasopharynx or ear, and the data are pooled from two replicate experiments. The short, solid horizontal lines indicate the geometric mean, and the dotted line represents the limit of detection of the assay. Statistical analysis was performed using a two-tailed Mann-Whitney *U* test (*, $P < 0.05$; ** $P < 0.01$; *** $P < 0.001$). (C and D) Correlations between nasal colonization density of *S. pneumoniae* and the middle ear pneumococcal titers in mice coinfected with IAV and either the opaque variant (C) or the transparent variant (D). Each ear is correlated to its respective nasopharynx. The data contain both time points and are pooled from two replicate experiments. Statistical analysis was performed using Spearman's rank correlation test and is denoted by Spearman's rank correlation coefficient (*r*) and *P* value.

infection, however, increased the nasal colonization of the opaque variant by 16-fold and that of the transparent variant by 11-fold. As a result, IAV coinfection ultimately removed the colonization defect of the opaque variant such that the nasal pneumococcal burden between the variants was indistinguishable at both days and 2 and 4 ($P = 0.81$ and $P = 0.38$, respectively) (Fig. 5A). Of note, IAV coinfection did not alter the pneumococcal phase composition in the nasopharynx or middle ears relative to singly infected mice, with the exception of a small but statistically significant increase in the proportion of opaque colonies in the nares of mice coinfected with IAV and the opaque variant at day 2 ($P = 0.0129$) (Table 2). Taken together, these results demonstrate that IAV coinfection overcomes inherent colonization deficits of the opaque phase, including reduced adherence and biofilm viability, ultimately enabling the opaque variant to colonize the nasopharynx at a level commensurate with its transparent counterpart.

Influenza virus exacerbates middle ear infection by both pneumococcal phases. We next sought to determine whether the increased nasal colonization by both phase variants following IAV infection altered the magnitude of middle ear infection. As the opaque phase has been shown to be isolated more frequently from the ears of children with OM (26), we were initially surprised to discover in singly infected mice that the numbers of pneumococci in the middle ears were similar between both phase variants (Fig. 5B). This finding likely stems from the colonizing strain used in this study, which has been shown to inherently disseminate poorly from the nasopharynx in the absence of external stimuli (37). During coinfection with IAV, middle ear infection by both the opaque and transparent variants was significantly increased relative to levels in singly infected mice. Interestingly, however, bacterial titers were similar between the phase variants (Fig. 5B). This similar magnitude of pneumococcal middle ear infection following IAV infection was not explained solely by phase shifting *in vivo*. Despite similar titers, colonies isolated from the ears of mice infected with the opaque variant remained 98.1 to 100% opaque while those from mice infected with the transparent variant were 22.8 to 26.4% opaque (Table 2).

Since we observed a correlation between nasal colonization density and middle ear infection with the parent EF3030 strain (Fig. 1C), we hypothesized that a similar mechanism would account for the equal magnitudes of middle ear infection by both phase variants following coinfection. To investigate this, the correlation between the nasopharyngeal bacterial density and the middle ear pneumococcal burden in each mouse was again assessed. In the absence of IAV, there was no significant correlation by either phase variant ($P > 0.05$, Spearman's rank correlation test [data not shown]). Following IAV infection, there was indeed a highly significant correlation between nasal colonization and the

resultant magnitude of middle ear infection with the opaque phase variant ($P < 0.001$, Spearman's rank correlation test) (Fig. 5C). Interestingly, no such relationship was observed during IAV coinfection with the transparent variant (Fig. 5D). This indicated that the increase in the magnitude of middle ear infection by the transparent variant was not due simply to greater nasal colonization density following IAV coinfection and that multiple factors are likely involved. Taken together, however, these findings establish that the influenza virus exacerbation of pneumococcal middle ear infection was phase independent. Further work is needed to investigate the mechanisms by which IAV enhances nasopharyngeal dissemination by both phases.

DISCUSSION

The importance of IAV in the induction of pneumococcal dissemination from the nasopharynx has been well studied. However, pneumococci are known to persist in the human nasopharynx as a mixture of two phases that differ in amounts of capsular polysaccharide and exposure of bacterial surface moieties (26, 33, 34). How these specifically interact with influenza virus in the context of middle ear infection is less appreciated.

In this study, we first established a murine model wherein a preexisting influenza A virus infection enhanced the nasopharyngeal colonization by a pneumococcal strain that naturally contains both phases. Prior work has shown that IAV can also enhance nasal colonization when given after pneumococcal inoculation (19). Together, these findings suggest that this synergism is likely occurring quite frequently as these pathogens are serially acquired and cleared. Indeed, children experience a median of seven carriage episodes before the age of 2 years and face an average of six respiratory viral infections each year (9, 50). The increased nasal colonization observed in our model following IAV infection correlated with an increased magnitude of middle ear pneumococcal infection, mirroring clinical data from children (44, 51). Of note, this finding regarding middle ear bacterial burden contradicted the findings of Short et al., who noted that the H1 hemagglutinin of IAV PR8/34 (H1N1) was unable to induce pneumococcal OM in infant C57BL/6 mice (21). This disparity is likely attributable to differences in both the ages and strains of the mice, particularly as the content of sialic acid, the hemagglutinin ligand, varies among mouse species (52). However, our findings in an adult murine model indicate that pneumococcal middle ear infection can also be exacerbated by H1N1 influenza virus, the most prevalent circulating subtype in the United States (53).

Using this model, we discovered the presence of viral RNA in the middle ears of a subset of both IAV- and coinfected mice. As qRT-PCR is not a direct measure of viral infectivity, it is possible that this simply represents contaminating viral RNA from the nasopharynx. This is a difficult question as there are contrasting opinions in the field regarding this subject (expertly reviewed in reference 54). However, in both children and animal models, viral infection of the middle ear has been linked to inflammation (21, 54). In this study, we detected IAV RNA and evidence of mucosal inflammation as late as 6 days post-viral infection in mice infected with IAV alone. Thus, it appears likely that in this model the presence of viral nucleic acid represents an infection. Supporting this hypothesis, we found that pneumococcal middle ear burden was greatest in IAV-infected ears. Clinically, this direct synergism in IAV-infected ears may account for the increased rates of antibiotic failure in OM cases where both bacteria and viruses are detected in the ear (55).

The mechanisms underpinning this IAV-pneumococcal synergism remain to be fully elucidated. From our findings, it seems apparent that the viral enhancement of bacterial colonization is a critical component. As adherence is required for pneumococci to form the surface-attached biofilms that are hallmarks of colonization (31, 32), the nasal epithelial changes we observed following IAV infection likely contribute to this process. In addition, IAV is known to expose specific pneumococcal binding sites through its neuraminidase activity (56) as well as potentially through the induction of epithelial platelet-activating factor expression (27). Recent work by Marks et al. suggests that in addition to increasing nasal colonization, influenza A virus also induces pneumococcal dissemination from the nasopharynx via changes to the host microenvironment, including hyperthermia and nutrient availability (57). Once translocated from the nasopharynx, the virally induced mucosal inflammation we observed in the middle ears of IAV-infected mice (and exacerbated by bacterial coinfection) can then itself contribute to the establishment of pneumococcal middle ear infection (21).

In light of these findings, an important question remains: is this IAV predisposition to enhanced middle ear infection by *S. pneumoniae* a uniform process that universally enables increased outgrowth and dissemination? The work of McCullers et al. began to answer this question and found that the IAV modulation of pneumococcal disease was bacterial strain dependent (14). Tong et al. further explored whether the intrastrain opaque and transparent phases are differentially affected by preceding IAV infection in a chinchilla model of OM (35). The authors' conclusions in that study complement our findings with one key distinction. Tong et al. similarly observed an increase in both nasal colonization and middle ear infection by both phase variants following IAV infection, ultimately to similar levels of bacterial burden at early time points. In contrast to our findings, however, Tong et al. did not observe a difference in inherent nasal colonization between the phase variants in the absence of viral infection (35). Thus, our findings further contribute the observation that IAV infection is sufficient to alter the nasopharyngeal microenvironment such that the opaque phase is capable of colonizing at a level similar to that of its transparent counterpart. This has significant implications as an invasive serotype, such as serotype 1, which is almost always found in invasive disease and rarely in nasal carriage, has been shown to be significantly more associated with the opaque phase (58). The discrepancy in the observed colonization by the opaque phase between this study and that by Tong et al. is likely accounted for by differences in the serotypes studied and in the animal models employed. Indeed, the distinction in virulence between the two phases has previously been shown to differ between animal species (25, 34).

The ablation of the colonizing defect of the opaque phase by IAV occurred despite the impaired epithelial adherence and biofilm viability that we observed *in vitro*. Previously, pneumococcal adherence to lower respiratory tract epithelial cells has been shown to increase following influenza A viral infection (59). Additionally, both phase variants have been shown to adhere via the receptor for platelet-activating factor, though to a greater extent by the transparent phase (27). As this specific receptor has been shown to be upregulated by rhinovirus infection (60), we hypothesize that influenza viral infection may have a similar effect,

thereby enabling nasal colonization to increase by both phases. Further, the expression and activity of the pneumococcal neuraminidase, critical for carriage, are diminished in the opaque phase (61, 62). As the IAV neuraminidase has been shown to synergistically interact with pneumococci (56), it is conceivable that the viral neuraminidase could complement the opaque phase. This area is in need of further study.

The opaque phase has been shown to more efficiently infect and persist in invasive sites such as the lungs and bloodstream in animal models (25, 63). While the middle ear is not generally considered an invasive site, we observed that middle ear infections were similar between the two phase variants following IAV coinfection. It is important to note, however, that studies characterizing the two phases were initially performed using more invasive strains derived from blood isolates (25, 34). As such, the distinction between phases may be more subtle in a colonizing strain such as EF3030 (25, 34, 36, 37). Reflecting this possibility, we did not observe an increase in the incidence or magnitude of middle ear infection by the opaque-phase variant in the absence of IAV. While similar numbers of the opaque and transparent variants were found in the middle ear during IAV coinfection, pneumococci within this site were still more frequently in the opaque phase than in the nasopharynx. This study could not distinguish whether this represented, in the case of the transparent variant, preferential expansion of the small subpopulation of opaque-phase bacteria in the inoculum or phase shifting *in vivo*. As pneumococcal phases vary at frequencies ranging from 10^{-3} to 10^{-7} per generation, it is likely that both are occurring and contributing to the similar magnitudes of middle ear infection by both phase variants.

Despite a similar magnitude of infection, the IAV exacerbation of pneumococcal middle ear infection by both phases appears to occur, in part, via divergent mechanisms. In the opaque phase, the enhanced middle ear infection is directly linked to the increased nasal colonization density induced by viral coinfection. This was reflected in our correlation data and is in agreement with the recent findings by Marks et al. that opaque-phase pneumococci disperse more readily from a biofilm state (57). In children, the incidence of OM is linked to nasal colonization density. Our findings thus further suggest that the opaque phase is primarily responsible for this clinically observed phenotype (44). As this correlation is absent during IAV coinfection with the transparent variant, additional factors beyond nasal colonization density are likely involved. Indeed, once the preceding viral infection enables transparent-phase pneumococci to ascend the eustachian tube, the increased adherence and biofilm viability that we observed *in vitro* can then enable this phase to increasingly infect the middle ear. Supporting this hypothesis, transparent-phase pneumococci have been shown to bind more readily to specific *N*-acetylglucosamine residues in the eustachian tube that are exposed by IAV (27, 64).

In summary, these results indicate that coinfection with influenza A virus increases both nasal and middle ear epithelial inflammation and that this is associated with significantly enhanced nasal colonization and middle ear infection by *S. pneumoniae*. Further, despite inherent differences in *in vitro* biofilm viability and adherence and *in vivo* colonization, this effect is independent of the predominant pneumococcal phase.

ACKNOWLEDGMENTS

This work was supported by National Institutes of Health, National Institute of Deafness and Other Communication Diseases (grant number R01 DC10051 to W.E.S.).

We gratefully thank Griffith D. Parks for propagating the influenza viral inocula determining the titers, John B. Johnson, Melissa B. Oliver, Li Tan, Jessie E. Wozniak, and Uma Ghandi for technical assistance with the mouse experiments, and Stephen H. Richardson for critical review of the manuscript.

We have no potential conflicts of interest to disclose.

REFERENCES

1. **Ahmed S, Shapiro NL, Bhattacharyya N.** 2014. Incremental health care utilization and costs for acute otitis media in children. Laryngoscope **124:** 301–305. http://dx.doi.org/10.1002/lary.24190.
2. **Rovers MM, Schilder AG, Zielhuis GA, Rosenfeld RM.** 2004. Otitis media. Lancet **363:**465–473. http://dx.doi.org/10.1016/S0140-6736(04)15495-0.
3. **Casey JR, Kaur R, Friedel VC, Pichichero ME.** 2013. Acute otitis media otopathogens during 2008 to 2010 in Rochester, New York. Pediatr. Infect. Dis. J. **32:**805–809. http://dx.doi.org/10.1097/INF.0b013e31828d9acc.
4. **Adegbola RA, Obaro SK, Biney E, Greenwood BM.** 2001. Evaluation of Binax Now *Streptococcus pneumoniae* urinary antigen test in children in a community with a high carriage rate of pneumococcus. Pediatr. Infect. Dis. J. **20:**718–719. http://dx.doi.org/10.1097/00006454-200107000-00018.
5. **Ghaffar F, Friedland IR, McCracken GH, Jr.** 1999. Dynamics of nasopharyngeal colonization by *Streptococcus pneumoniae*. Pediatr. Infect. Dis. J. **18:**638–646. http://dx.doi.org/10.1097/00006454-199907000-00016.
6. **Gray BM, Converse GM, III, Dillon HC, Jr.** 1980. Epidemiologic studies of *Streptococcus pneumoniae* in infants: acquisition, carriage, and infection during the first 24 months of life. J. Infect. Dis. **142:**923–933. http://dx.doi.org/10.1093/infdis/142.6.923.
7. **Heikkinen T, Chonmaitree T.** 2003. Importance of respiratory viruses in acute otitis media. Clin. Microbiol. Rev. **16:**230–241. http://dx.doi.org/10.1128/CMR.16.2.230-241.2003.
8. **Chonmaitree T.** 2000. Viral and bacterial interaction in acute otitis media. Pediatr. Infect. Dis. J. **19:**S24–S30. http://dx.doi.org/10.1097/00006454-200005001-00005.
9. **Chonmaitree T, Revai K, Grady JJ, Clos A, Patel JA, Nair S, Fan J, Henrickson KJ.** 2008. Viral upper respiratory tract infection and otitis media complication in young children. Clin. Infect. Dis. **46:**815–823. http://dx.doi.org/10.1086/528685.
10. **Heikkinen T.** 2000. The role of respiratory viruses in otitis media. Vaccine **19**(Suppl 1):S51–S55. http://dx.doi.org/10.1016/S0264-410X(00)00278-4.
11. **Ruohola A, Pettigrew MM, Lindholm L, Jalava J, Raisanen KS, Vainionpaa R, Waris M, Tahtinen PA, Laine MK, Lahti E, Ruuskanen O, Huovinen P.** 2013. Bacterial and viral interactions within the nasopharynx contribute to the risk of acute otitis media. J. Infect. **66:**247–254. http://dx.doi.org/10.1016/j.jinf.2012.12.002.
12. **Buchman CA, Doyle WJ, Skoner DP, Post JC, Alper CM, Seroky JT, Anderson K, Preston RA, Hayden FG, Fireman P, Ehrlich GD.** 1995. Influenza A virus-induced acute otitis media. J. Infect. Dis. **172:**1348–1351. http://dx.doi.org/10.1093/infdis/172.5.1348.
13. **Wadowsky RM, Mietzner SM, Skoner DP, Doyle WJ, Fireman P.** 1995. Effect of experimental influenza A virus infection on isolation of *Streptococcus pneumoniae* and other aerobic bacteria from the oropharynges of allergic and nonallergic adult subjects. Infect. Immun. **63:**1153–1157.
14. **McCullers JA, McAuley JL, Browall S, Iverson AR, Boyd KL, Henriques Normark B.** 2010. Influenza enhances susceptibility to natural acquisition of and disease due to *Streptococcus pneumoniae* in ferrets. J. Infect. Dis. **202:**1287–1295. http://dx.doi.org/10.1086/656333.
15. **Giebink GS.** 1989. Studies of *Streptococcus pneumoniae* and influenza virus vaccines in the chinchilla otitis media model. Pediatr. Infect. Dis. J. **8:**S42–S44. http://dx.doi.org/10.1097/00006454-198901001-00016.
16. **Giebink GS, Wright PF.** 1983. Different virulence of influenza A virus strains and susceptibility to pneumococcal otitis media in chinchillas. Infect. Immun. **41:**913–920.
17. **Stol K, van Selm S, van den Berg S, Bootsma HJ, Blokx WA, Graamans K, Tonnaer EL, Hermans PW.** 2009. Development of a non-invasive murine infection model for acute otitis media. Microbiology **155:**4135–4144. http://dx.doi.org/10.1099/mic.0.033175-0.

18. **MacArthur CJ, Hefeneider SH, Kempton JB, Parrish SK, McCoy SL, Trune DR.** 2006. Evaluation of the mouse model for acute otitis media. Hear. Res. **219:**12–23. http://dx.doi.org/10.1016/j.heares.2006.05.012.
19. **Diavatopoulos DA, Short KR, Price JT, Wilksch JJ, Brown LE, Briles DE, Strugnell RA, Wijburg OL.** 2010. Influenza A virus facilitates *Streptococcus pneumoniae* transmission and disease. FASEB J. **24:**1789–1798. http://dx.doi.org/10.1096/fj.09-146779.
20. **Short KR, Diavatopoulos DA, Thornton R, Pedersen J, Strugnell RA, Wise AK, Reading PC, Wijburg OL.** 2011. Influenza virus induces bacterial and nonbacterial otitis media. J. Infect. Dis. **204:**1857–1865. http://dx.doi.org/10.1093/infdis/jir618.
21. **Short KR, Reading PC, Brown LE, Pedersen J, Gilbertson B, Job ER, Edenborough KM, Habets MN, Zomer A, Hermans PW, Diavatopoulos DA, Wijburg OL.** 2013. Influenza-induced inflammation drives pneumococcal otitis media. Infect. Immun. **81:**645–652. http://dx.doi.org/10.1128/IAI.01278-12.
22. **Abramson JS, Lyles DS, Heller KA, Bass DA.** 1982. Influenza A virus-induced polymorphonuclear leukocyte dysfunction. Infect. Immun. **37:**794–799.
23. **Julkunen I, Melen K, Nyqvist M, Pirhonen J, Sareneva T, Matikainen S.** 2000. Inflammatory responses in influenza A virus infection. Vaccine **19**(Suppl 1):S32–S37. http://dx.doi.org/10.1016/S0264-410X(00)00275-9.
24. **Park K, Bakaletz LO, Coticchia JM, Lim DJ.** 1993. Effect of influenza A virus on ciliary activity and dye transport function in the chinchilla eustachian tube. Ann. Otol. Rhinol. Laryngol. **102:**551–558.
25. **Weiser JN, Austrian R, Sreenivasan PK, Masure HR.** 1994. Phase variation in pneumococcal opacity: relationship between colonial morphology and nasopharyngeal colonization. Infect. Immun. **62:**2582–2589.
26. **Arai J, Hotomi M, Hollingshead SK, Ueno Y, Briles DE, Yamanaka N.** 2011. *Streptococcus pneumoniae* isolates from middle ear fluid and nasopharynx of children with acute otitis media exhibit phase variation. J. Clin. Microbiol. **49:**1646–1649. http://dx.doi.org/10.1128/JCM.01990-10.
27. **Cundell DR, Weiser JN, Shen J, Young A, Tuomanen EI.** 1995. Relationship between colonial morphology and adherence of *Streptococcus pneumoniae*. Infect. Immun. **63:**757–761.
28. **Sanchez CJ, Kumar N, Lizcano A, Shivshankar P, Dunning Hotopp JC, Jorgensen JH, Tettelin H, Orihuela CJ.** 2011. *Streptococcus pneumoniae* in biofilms are unable to cause invasive disease due to altered virulence determinant production. PLoS One **6:**e28738. http://dx.doi.org/10.1371/journal.pone.0028738.
29. **Donlan RM.** 2002. Biofilms: microbial life on surfaces. Emerg. Infect. Dis. **8:**881–890. http://dx.doi.org/10.3201/eid0809.020063.
30. **Munoz-Elias EJ, Marcano J, Camilli A.** 2008. Isolation of *Streptococcus pneumoniae* biofilm mutants and their characterization during nasopharyngeal colonization. Infect. Immun. **76:**5049–5061. http://dx.doi.org/10.1128/IAI.00425-08.
31. **Marks LR, Parameswaran GI, Hakansson AP.** 2012. Pneumococcal interactions with epithelial cells are crucial for optimal biofilm formation and colonization in vitro and in vivo. Infect. Immun. **80:**2744–2760. http://dx.doi.org/10.1128/IAI.00488-12.
32. **Reid SD, Hong W, Dew KE, Winn DR, Pang B, Watt J, Glover DT, Hollingshead SK, Swords WE.** 2009. *Streptococcus pneumoniae* forms surface-attached communities in the middle ear of experimentally infected chinchillas. J. Infect. Dis. **199:**786–794. http://dx.doi.org/10.1086/597042.
33. **Kim JO, Romero-Steiner S, Sorensen UB, Blom J, Carvalho M, Barnard S, Carlone G, Weiser JN.** 1999. Relationship between cell surface carbohydrates and intrastrain variation on opsonophagocytosis of *Streptococcus pneumoniae*. Infect. Immun. **67:**2327–2333.
34. **Kim JO, Weiser JN.** 1998. Association of intrastrain phase variation in quantity of capsular polysaccharide and teichoic acid with the virulence of *Streptococcus pneumoniae*. J. Infect. Dis. **177:**368–377. http://dx.doi.org/10.1086/514205.
35. **Tong HH, Weiser JN, James MA, DeMaria TF.** 2001. Effect of influenza A virus infection on nasopharyngeal colonization and otitis media induced by transparent or opaque phenotype variants of *Streptococcus pneumoniae* in the chinchilla model. Infect. Immun. **69:**602–606. http://dx.doi.org/10.1128/IAI.69.1.602-606.2001.
36. **Andersson B, Dahmen J, Frejd T, Leffler H, Magnusson G, Noori G, Eden CS.** 1983. Identification of an active disaccharide unit of a glycoconjugate receptor for pneumococci attaching to human pharyngeal epithelial cells. J. Exp. Med. **158:**559–570. http://dx.doi.org/10.1084/jem.158.2.559.
37. **Briles DE, Crain MJ, Gray BM, Forman C, Yother J.** 1992. Strong association between capsular type and virulence for mice among human isolates of *Streptococcus pneumoniae*. Infect. Immun. **60:**111–116.
38. **Manicassamy B, Manicassamy S, Belicha-Villanueva A, Pisanelli G, Pulendran B, Garcia-Sastre A.** 2010. Analysis of in vivo dynamics of influenza virus infection in mice using a GFP reporter virus. Proc. Natl. Acad. Sci. U. S. A. **107:**11531–11536. http://dx.doi.org/10.1073/pnas.0914994107.
39. **Briles DE, Novak L, Hotomi M, van Ginkel FW, King J.** 2005. Nasal colonization with *Streptococcus pneumoniae* includes subpopulations of surface and invasive pneumococci. Infect. Immun. **73:**6945–6951. http://dx.doi.org/10.1128/IAI.73.10.6945-6951.2005.
40. **CDC.** 2008. Human influenza virus real-time RT-PCR detection and characterization panel 510(k). CDC, Atlanta, GA. http://www.accessdata.fda.gov/cdrh_docs/pdf8/k080570.pdf.
41. **van Elden LJ, Nijhuis M, Schipper P, Schuurman R, van Loon AM.** 2001. Simultaneous detection of influenza viruses A and B using real-time quantitative PCR. J. Clin. Microbiol. **39:**196–200. http://dx.doi.org/10.1128/JCM.39.1.196-200.2001.
42. **Gould JM, Weiser JN.** 2002. The inhibitory effect of C-reactive protein on bacterial phosphorylcholine platelet-activating factor receptor-mediated adherence is blocked by surfactant. J. Infect. Dis. **186:**361–371. http://dx.doi.org/10.1086/341658.
43. **Perez AC, Pang B, King LB, Tan L, Murrah KA, Reimche JL, Wren JT, Richardson SH, Ghandi U, Swords WE.** 2014. Residence of *Streptococcus pneumoniae* and *Moraxella catarrhalis* within polymicrobial biofilm promotes antibiotic resistance and bacterial persistence in vivo. Pathog. Dis. **70:**280–288. http://dx.doi.org/10.1111/2049-632X.12129.
44. **Smith-Vaughan H, Byun R, Nadkarni M, Jacques NA, Hunter N, Halpin S, Morris PS, Leach AJ.** 2006. Measuring nasal bacterial load and its association with otitis media. BMC Ear Nose Throat Disord. **6:**10. http://dx.doi.org/10.1186/1472-6815-6-10.
45. **Rovers MM, Glasziou P, Appelman CL, Burke P, McCormick DP, Damoiseaux RA, Gaboury I, Little P, Hoes AW.** 2006. Antibiotics for acute otitis media: a meta-analysis with individual patient data. Lancet **368:**1429–1435. http://dx.doi.org/10.1016/S0140-6736(06)69606-2.
46. **Weiser JN.** 2010. The pneumococcus: why a commensal misbehaves. J. Mol. Med. (Berl.) **88:**97–102. http://dx.doi.org/10.1007/s00109-009-0557-x.
47. **Sato K, Liebeler CL, Quartey MK, Le CT, Giebink GS.** 1999. Middle ear fluid cytokine and inflammatory cell kinetics in the chinchilla otitis media model. Infect. Immun. **67:**1943–1946.
48. **Salvinelli F, Greco F, Trivelli M, Linthicum FH, Jr.** 1999. Acute otitis media. Histopathological changes: a post mortem study on temporal bones. Eur. Rev. Med. Pharmacol. Sci. **3:**75–79.
49. **Sekhar S, Kumar R, Chakraborti A.** 2009. Role of biofilm formation in the persistent colonization of *Haemophilus influenzae* in children from northern India. J. Med. Microbiol. **58:**1428–1432. http://dx.doi.org/10.1099/jmm.0.010355-0.
50. **Turner P, Turner C, Jankhot A, Helen N, Lee SJ, Day NP, White NJ, Nosten F, Goldblatt D.** 2012. A longitudinal study of *Streptococcus pneumoniae* carriage in a cohort of infants and their mothers on the Thailand-Myanmar border. PLoS One **7:**e38271. http://dx.doi.org/10.1371/journal.pone.0038271.
51. **Bernstein JM, Faden HF, Dryja DM, Wactawski-Wende J.** 1993. Microecology of the nasopharyngeal bacterial flora in otitis-prone and non-otitis-prone children. Acta Otolaryngol. **113:**88–92. http://dx.doi.org/10.3109/00016489309135772.
52. **Kato K, Takegawa Y, Ralston KS, Gilchrist CA, Hamano S, Petri WA, Jr, Shinohara Y.** 2013. Sialic acid-dependent attachment of mucins from three mouse strains to *Entamoeba histolytica*. Biochem. Biophys. Res. Commun. **436:**252–258. http://dx.doi.org/10.1016/j.bbrc.2013.05.085.
53. **CDC.** 2014. FluView: 2013-2014 influenza season, week 24 ending June 14, 2014. CDC, Atlanta, GA.
54. **Chonmaitree T, Ruohola A, Hendley JO.** 2012. Presence of viral nucleic acids in the middle ear: acute otitis media pathogen or bystander? Pediatr. Infect. Dis. J. **31:**325–330. http://dx.doi.org/10.1097/INF.0b013e318241afe4.
55. **Chonmaitree T, Owen MJ, Patel JA, Hedgpeth D, Horlick D, Howie VM.** 1992. Effect of viral respiratory tract infection on outcome of acute otitis media. J. Pediatr. **120:**856–862. http://dx.doi.org/10.1016/S0022-3476(05)81950-X.
56. **McCullers JA, Bartmess KC.** 2003. Role of neuraminidase in lethal synergism between influenza virus and *Streptococcus pneumoniae*. J. Infect. Dis. **187:**1000–1009. http://dx.doi.org/10.1086/368163.
57. **Marks LR, Davidson BA, Knight PR, Hakansson AP.** 2013. Interking-

dom signaling induces *Streptococcus pneumoniae* biofilm dispersion and transition from asymptomatic colonization to disease. mBio **4**(4)**:**e00438-13. http://dx.doi.org/10.1128/mBio.00438-13.

58. **Serrano I, Melo-Cristino J, Ramirez M.** 2006. Heterogeneity of pneumococcal phase variants in invasive human infections. BMC Microbiol. **6:**67. http://dx.doi.org/10.1186/1471-2180-6-67.
59. **Avadhanula V, Rodriguez CA, Devincenzo JP, Wang Y, Webby RJ, Ulett GC, Adderson EE.** 2006. Respiratory viruses augment the adhesion of bacterial pathogens to respiratory epithelium in a viral species- and cell type-dependent manner. J. Virol. **80:**1629–1636. http://dx.doi.org/10.1128/JVI.80.4.1629-1636.2006.
60. **Ishizuka S, Yamaya M, Suzuki T, Takahashi H, Ida S, Sasaki T, Inoue D, Sekizawa K, Nishimura H, Sasaki H.** 2003. Effects of rhinovirus infection on the adherence of *Streptococcus pneumoniae* to cultured human airway epithelial cells. J. Infect. Dis. **188:**1928–1939. http://dx.doi.org/10.1086/379833.
61. **King SJ, Hippe KR, Gould JM, Bae D, Peterson S, Cline RT, Fasching C, Janoff EN, Weiser JN.** 2004. Phase variable desialylation of host proteins that bind to *Streptococcus pneumoniae* in vivo and protect the airway. Mol. Microbiol. **54:**159–171. http://dx.doi.org/10.1111/j.1365-2958.2004.04252.x.
62. **Tong HH, Blue LE, James MA, DeMaria TF.** 2000. Evaluation of the virulence of a *Streptococcus pneumoniae* neuraminidase-deficient mutant in nasopharyngeal colonization and development of otitis media in the chinchilla model. Infect. Immun. **68:**921–924. http://dx.doi.org/10.1128/IAI.68.2.921-924.2000.
63. **Weiser JN.** 1998. Phase variation in colony opacity by *Streptococcus pneumoniae*. Microb. Drug Resist. **4:**129–135. http://dx.doi.org/10.1089/mdr.1998.4.129.
64. **Tong HH, Grants I, Liu X, DeMaria TF.** 2002. Comparison of alteration of cell surface carbohydrates of the chinchilla tubotympanum and colonial opacity phenotype of *Streptococcus pneumoniae* during experimental pneumococcal otitis media with or without an antecedent influenza A virus infection. Infect. Immun. **70:**4292–4301. http://dx.doi.org/10.1128/IAI.70.8.4292-4301.2002.